

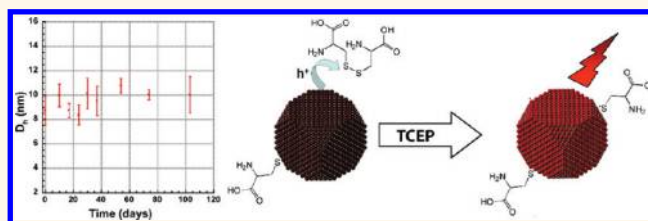
Aqueous Phase Transfer of InP/ZnS Nanocrystals Conserving Fluorescence and High Colloidal Stability

Sudarsan Tamang,[†] Grégory Beaune,^{†,‡} Isabelle Texier,[‡] and Peter Reiss^{†,*}

[†]CEA-Grenoble, INAC-SPRAM (UMR 5819 CEA-CNRS-UJF)-LEMOH, 17 Rue des Martyrs, 38054 Grenoble Cedex 9, France, and [‡]CEA-Grenoble, LETI-DTBS, 17 Rue des Martyrs, 38054 Grenoble Cedex 9, France

The transfer of fluorescent semiconductor nanocrystals (NCs) or quantum dots (QDs) prepared in organic solvents to the aqueous phase is an essential step for benefiting from the progress of nanoscience in biotechnology.^{1–3} The basic requirement of a given phase transfer reaction is the colloidal stability of the QDs in aqueous environment over an extended period of time. One way to address this issue is the use of specially designed organic ligands—a strategy that has also been successfully applied to gold and silver nanoparticles (NPs). Mono- and dithioalkylated polyethylene glycols,^{4,5} peptide-based ligands,^{6,7} phospholipid micelles,⁸ and amphiphilic polymers⁹ have been used with the goal to prevent particle aggregation after phase transfer. Despite remarkable stability in aqueous environment of various NCs and NPs capped with these engineered ligands, the small amino acid cysteine has recently also drawn strong attention, mainly due to its zwitterionic nature, compact size, and commercial availability.¹⁰ Both cationic and anionic ligands exhibit nonspecific interactions with serum proteins, resulting in an increased hydrodynamic diameter (D_h). In contrast, NCs coated with zwitterionic ligands have been shown to produce small hydrodynamic diameters ($D_h \sim 5–10$ nm).¹¹ For both *in vitro* and *in vivo* studies, the compact size of the used fluorescent probes can be mandatory. Examples are monitoring the traffic within synapses,¹² extravagation of QDs from vasculature,¹³ and renal clearance, observed in mice.¹⁰ In the latter case, very compact ($D_h \sim 6$ nm) cysteine-capped CdSe/CdZnS NCs have been applied, which have been transferred to the aqueous phase with cysteine at physiological pH (7.4). However, these NCs were found to be stable only for 24 h at 4 °C before their precipitation occurred.¹¹ The

ABSTRACT



Small thiol-containing amino acids such as cysteine are appealing surface ligands for transferring semiconductor quantum dots (QDs) from organic solvents to the aqueous phase. They provide a compact hydrodynamic diameter and low nonspecific binding in biological environment. However, cysteine-capped QDs generally exhibit modest colloidal stability in water and their fluorescence quantum yield (QY) is significantly reduced as compared to organics. We demonstrate that during phase transfer the deprotonation of the thiol group by carefully adjusting the pH is of crucial importance for increasing the binding strength of cysteine to the QD surface. As a result, the colloidal stability of cysteine-capped InP/ZnS core/shell QDs is extended from less than one day to several months. The developed method is of very general character and can be used also with other hydrophilic thiols and various other types of QDs, e.g., CdSe/CdS/ZnS and CuInS₂/ZnS QDs as well as CdSe and CdSe/CdS nanorods. We show that the observed decrease of QY upon phase transfer with cysteine is related to the generation of cysteine dimer, cystine. This side-reaction implies the formation of disulfide bonds, which efficiently trap photogenerated holes and inhibit radiative recombination. On the other hand, this process is not irreversible. By addition of an appropriate reducing agent, tris(2-carboxyethyl)phosphine hydrochloride (TCEP), the QY can be partially recovered. When TCEP is already added during the phase transfer, the QY of cysteine-capped InP/ZnS QDs can be maintained almost quantitatively. Finally, we show that penicillamine is a promising alternative to cysteine for the phase transfer of QDs, as it is much less prone to disulfide formation.

KEYWORDS: quantum dots · nanocrystals · aqueous phase transfer · cysteine · penicillamine · fluorescence quantum yield

colloidal stability could be increased to one week by adding sodium borohydroxide and dithiothreitol (DTT), reducing agents that prevent ligand desorption triggered by disulfide formation. A more recent approach applies Zn complexes of the phase transfer ligands (dihydrolipoic acid or cysteine), which led to an increase of the

* Address correspondence to peter.reiss@cea.fr.

Received for review March 1, 2011 and accepted October 28, 2011.

Published online October 28, 2011
10.1021/nn203598c

© 2011 American Chemical Society

colloidal stability of CdSe/ZnS QDs from one day to three months.¹⁴

In addition to colloidal stability, the phase transfer of fluorescent semiconductor NCs into water should also maintain their fluorescence quantum yield (QY). The decrease of QY upon hydrosolubilization is commonly reported for both core as well as core/shell semiconductor NCs, such as CdSe/ZnS,^{3,14,15} CdSe/ZnCdS,^{10,11} and InP/ZnS.¹⁶ These results show that despite the protective inorganic shell, the fluorescence properties of the core can still be influenced by the surrounding medium in solution (*e.g.*, nature of organic capping ligands, pH). Quenching in the presence of an inorganic shell has been attributed to defects in the shell or to its insufficient thickness.¹⁵ The loss of fluorescence becomes a major issue when dealing with new classes of cadmium-free semiconductor NCs. These are generally less fluorescent than established Cd-based QDs, whose QY has been reported to reach almost 100% in organic solvents.^{17–19} InP/ZnS core/shell nanocrystals, for example, have attracted much interest as an alternative to Cd chalcogenide QDs.^{20–23} Conservation of PL QY and long-term stability have been reported by Xie *et al.* upon phase transfer of InP/ZnS QDs with thioglycolic acid at pH 10. However, no further details can be found in this work²⁰ or in a follow-up article. Using InP-based NCs, near-infrared (NIR) emission can be accessed at low size regime (<5 nm) due to the smaller band gap (1.35 eV) as compared to CdSe (1.75 eV) and comparable Bohr exciton radius. In addition to their potentially nontoxic character, this feature makes them especially appealing for *in vivo* studies.

In this article we present a generic method for the aqueous phase transfer of InP/ZnS QDs using various small hydrophilic thiols as transfer agents. We also show that this method works in principle for any type of QDs having an affinity for thiolated ligands. We address in particular the problems of colloidal stability and conservation of fluorescence. For all phase transfer agents studied, the deprotonation of the thiol function by appropriately adjusting the pH of the aqueous phase is of prime importance to obtain strong ligand binding to the NCs' surface. The versatility of the approach is demonstrated by successfully phase transferring CdSe nanospheres and nanorods as well as CdSe/CdS (spherical core/elongated shell) nanorods, CuInSe₂ core, CuInS₂/ZnS core/shell, and CdSe/CdS/ZnS core/shell/shell NCs in addition to InP and InP/ZnS QDs. Finally, we elucidate the origin of fluorescence quenching of cysteine-capped QDs, which is related to cysteine dimer (cystine) formation. We show that this problem can be solved by the addition of the reducing agent tris(2-carboxyethyl)phosphine hydrochloride (TCEP) during the phase transfer. On the other hand, our study confirms recent results of Breus *et al.*²⁴ showing that penicillamine—a molecule less

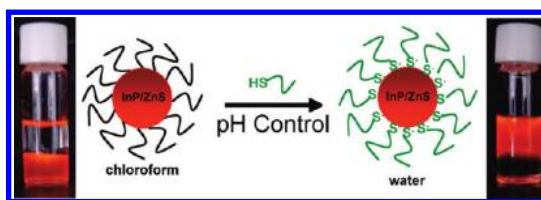


Figure 1. Phase transfer of InP/ZnS NCs in the presence of a hydrophilic thiolated ligand at a pH conducive for the deprotonation of the thiol group. The photographs show the NCs in chloroform before and in water after the phase transfer under UV light.

TABLE 1. Thiol pK_a Values for Each Ligand, Reaction pH Used for the Phase Transfer, Transfer Yield (amount of QDs in water/amount of QDs in chloroform), and Zeta Potential Measured in $1\times$ PBS Buffer for the Phase Transferred QDs

ligand	thiol pK_a	reaction pH (± 0.2)	transfer yield (%)	zeta potential (mV)
DHLA	10.7	11.9	89	-32.4 ± 4.3
Cys	8.35	9.3	60	-22.3 ± 0.7
TGA	9.78	10.3	74	-10.7 ± 1
MPA	10.8	11	78	-40.9 ± 1.7
MUA	~ 11	11.6	98	-36.5 ± 0.7

prone to dimerization than cysteine—constitutes an interesting alternative transfer agent in view of biological applications.

RESULTS AND DISCUSSIONS

Phase Transfer and Colloidal Stability. Phase transfer of InP/ZnS NCs is achieved by vigorously stirring a biphasic mixture of the QDs in chloroform and of the thiol-containing ligand in basic aqueous solution (Figure 1).

Our strategy to improve the colloidal stability of the NCs in water is based on the fact that the binding energy of thiolated ions to cations at the NCs' surface is much higher than the binding energy of the thiol group. For example, in the case of CdSe the calculated binding energies under vacuum for the thiolate and the thiol groups are 1283 and 34.7 kJ/mol, respectively.²⁵ Similarly, in the case of the shell material zinc sulfide, a relatively high binding energy has been reported for Zn–S_{thiolate} (194.7 kJ/mol), while S–S_{thiolate} and Zn–S_{thiol} account for 105.1 and 31.8 kJ/mol, respectively.²⁶ Since thiolate formation is pH dependent, the control of the pH during the phase transfer is of primary importance. The reaction pH should be chosen high enough (typically 8–11) for the deprotonation of the thiol group. On the other hand, basic pH values favor undesired disulfide formation. In this context we note that deprotonation of the thiol groups at neutral pH by stearate molecules desorbing from the NCs' surface is unlikely. Such a dynamic exchange has been observed in the case of oleate-capped CdSe NCs in the presence of free oleic acid in toluene.²⁷ However, in our case, given the pK_a values of stearic acid (5.0) and of the thiol functions of

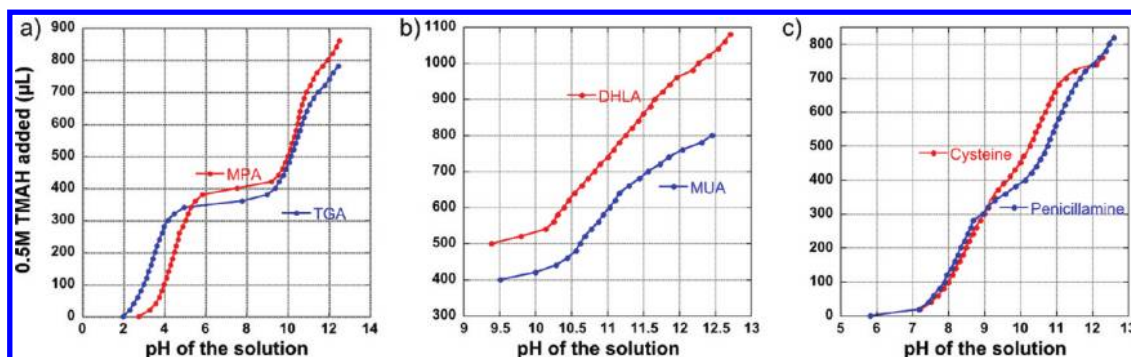
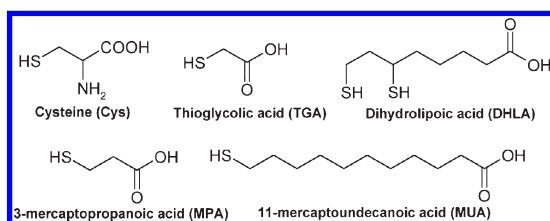


Figure 2. Titration curves of (a) 3-mercaptopropanoic acid (MPA) and thioglycolic acid (TGA); (b) 11-mercaptoundecanoic acid (MUA) and dihydroliipoic acid (DHLA); (c) L-cysteine and D-penicillamine. All compounds are used in 0.2 M aqueous solution, and a 0.5 M solution of tetramethylammonium hydroxide (TMAH) is added as the base. N.B.: MUA and DHLA are not soluble in the acidic or neutral pH range.



Scheme 1. Structures and abbreviations of the used ligands for aqueous phase transfer.

the phase transfer ligands (>8, *cf.* Table 1), the acid–base equilibrium $R-SH + R'-COO^- \leftrightarrow R-S^- + R'-COOH$ is strongly shifted to the left side. To determine the optimal pH for the phase transfer reaction, acid–base titration curves have been acquired by titrating a solution of each ligand against tetramethylammonium hydroxide, TMAH (Figure 2). The following ligands have been investigated (Scheme 1): cysteine (Cys), dihydroliipoic acid (DHLA), thioglycolic acid (TGA), 3-mercaptopropanoic acid (MPA), and 11-mercaptoundecanoic acid (MUA); the use of penicillamine (Pen) will be discussed in the second part of the paper.

The used pH values for the different transfer ligands are shown in Table 1. They are estimated from titration curves and/or derived from tabulated thiol dissociation constants.^{28–33}

The chosen ligand to QD ratio during the transfer reaction was 10^4 to 10^5 . Lower ligand:QD ratios (10^3 or 10^2) generally produced an increase of the mean D_h . For example, using cysteine as the transfer ligand for 660 nm emitting InP/ZnS QDs (inorganic diameter 5–6 nm), D_h values obtained from dynamic light scattering (DLS) measurements were around 8 nm for ligand:QD ratios of 10^5 and 10^4 , while using a ratio of 10^2 led to almost 11 nm (Table 2). Also, the QDs transferred with lower ligand concentration (samples 1 and 2) aggregated during the purification process, indicating incomplete ligand exchange.

During the phase transfer reaction, the QDs moved quantitatively from the organic to the aqueous phase within two hours, as could be judged from the color

TABLE 2. Hydrodynamic Diameter of 660 nm Emitting InP/ZnS NCs Transferred Using Different Ligand:QD Ratios^a

sample no.	[ligand]/[QD]	hydrodynamic diameter (nm)
1	100	10.7 ± 1.7
2	1000	9.6 ± 0.8
3	10 000	7.5 ± 2.6
4	100 000	7.9 ± 1.3

^aLigand = cysteine; mean value and standard deviation of 4 or 5 measurements.

changes of both phases. To assess the efficiency of the transfer process, the transfer yield was calculated for the QDs after purification. In fact, the fraction of QDs having an insufficient surface coverage with the new hydrophilic ligands could not be redispersed in water or buffer solution. Therefore the transfer yield is always below 100% and depends on the nature of the transfer ligand as well as on the bond strength of the original ligands on the NCs' surface. To calculate the transfer yield, the concentration of the samples before and after phase transfer is estimated from the first excitonic peak in the UV–vis spectra using the empirical correlations between the excitonic peak, size, and molar extinction coefficient compiled in ref 34. The obtained values varied from 60% to 98% for the different ligands (Table 1).

The QDs in aqueous media exhibit negative surface charge, as indicated by the zeta potential values in Table 1. We note that also zwitterionic cysteine leads to a negative surface charge at neutral pH. This result contradicts ref 11, where charge neutrality is claimed, but can easily be explained by the fact that the isoelectric point of cysteine lies at pH 5.0. It also implies that the absence of surface charge may not necessarily be at the origin of the observed reduced nonspecific binding of cysteine in biological environment.^{10,11} In the present study, surface charge together with the high binding energy of thiolated molecules on the InP/ZnS NCs' surface result in a remarkable colloidal stability of the QDs in aqueous

medium. Figure 3 shows the hydrodynamic diameter of the obtained cysteine-capped NCs in $1 \times$ PBS buffer at pH 7.4 plotted as a function of time. Within the experimental limits, during more than three months no size increase was observed. It should also be noted here that no additional reducing agent such as DTT was added to protect from cysteine oxidation, which has been attributed to trigger NCs' aggregation in earlier reports.¹¹

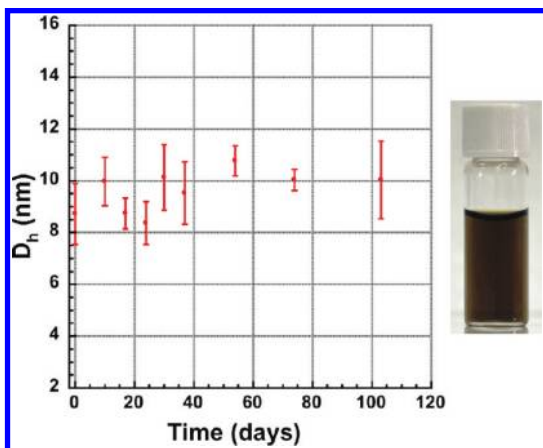


Figure 3. Stability of cysteine-capped InP/ZnS NCs in $1 \times$ PBS buffer illustrated by monitoring their hydrodynamic diameter as a function of time (TEM diameter 5–6 nm). The error bars indicate the standard deviation obtained for four or five measurements. Right: photograph of the colloidal solution after three months.

Conservation of Photoluminescence. Consistent with earlier reports,^{5,11,12,15,16,18} the phase transfer by means of surface ligand exchange is generally accompanied by a clear decrease of the fluorescence intensity. In Figure 4a the integrated photoluminescence is plotted against absorbance, which gives a direct comparison of the QY by comparing the slopes of the different curves. In our studies an unusually pronounced quenching was seen in the case of cysteine and DHLA, retaining only around 4% and 11%, respectively, of the initial PL intensity obtained with stearic acid (SA) ligands. TGA (~42%), MPA (~34%), and MUA (~26%) capped NCs were comparably brighter, as can be directly seen when the samples are put under a UV lamp (Figure 4b). Looking at these results and the transfer yields in Table 1, it is not surprising that simple mercaptocarboxylic acids such as TGA and MPA have been intensively studied as QDs' surface ligands in biological applications for a long time. To give an example, even the very first report on biological labeling with QDs in 1998 used MPA.² However, a large number of studies also showed that the solubility of QDs capped with this type of molecules is strongly limited at neutral or acidic pH and that they provoke nonspecific binding in a biological environment.^{10,11,24,29,35} As a consequence, aggregation of QDs in solution or inside cells is frequently observed. On the contrary zwitterionic ligands such as cysteine, carrying both positively and

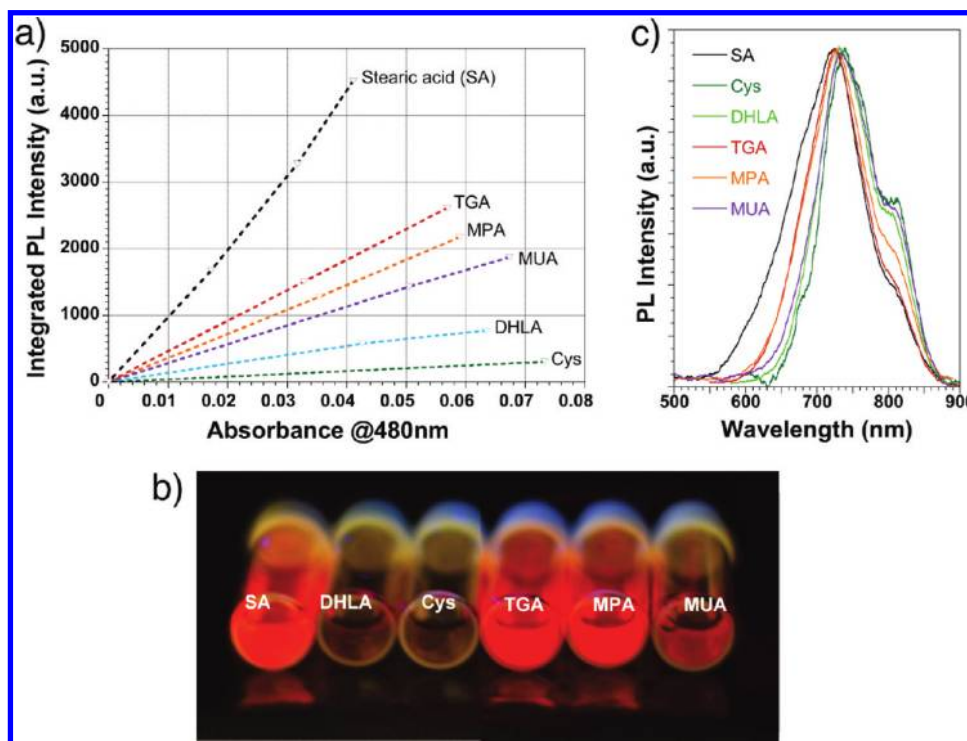


Figure 4. (a) Integrated photoluminescence vs absorbance plot for NCs capped with the different ligands in water (TGA, MPA, MUA, DHLA, Cys) and in hexane (SA). Absorbance is measured at 480 nm. Straight lines are added to guide the eye. (b) Photograph showing the obtained colloidal solutions under UV light (365 nm). (c) Normalized PL spectra of these samples ($\lambda_{\text{ex}} = 480$ nm).

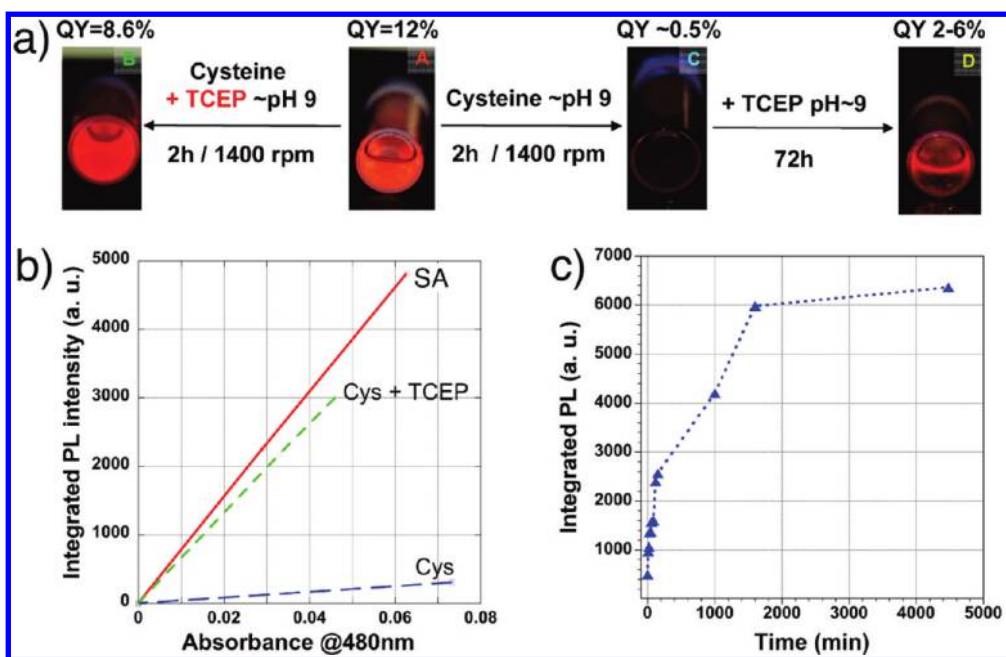
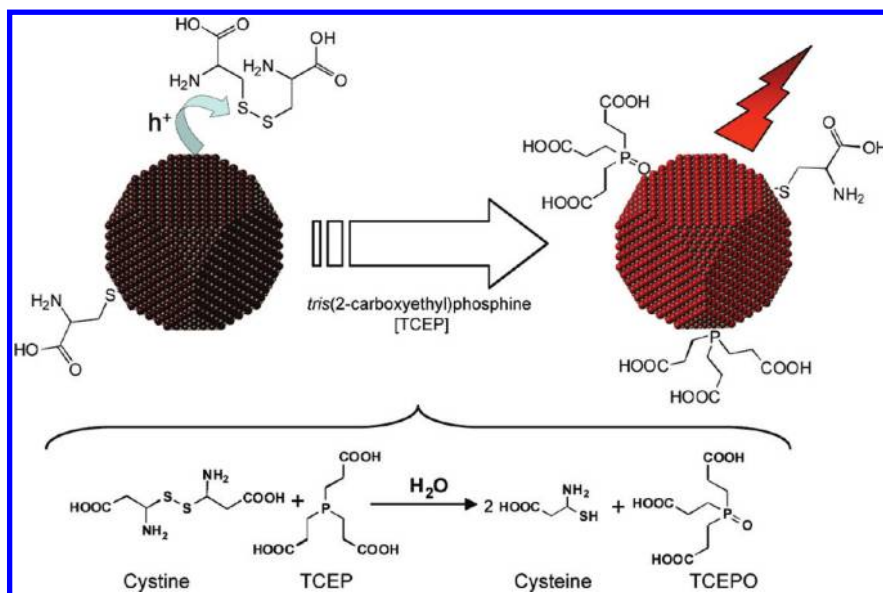


Figure 5. (a) Phase transfer of InP/ZnS NCs (A) at pH ~ 9 with cysteine in the presence (B) and in the absence (C) of TCEP; (D) fluorescence recovery by addition of 0.5 equiv (with respect to cysteine) of TCEP. (b) Integrated PL intensities as a function of absorbance for the samples A, B, and C. (c) Evolution of the relative PL intensity with time after TCEP addition (sample D).

negatively charged functional groups, are capable of providing much better colloidal stability at various pH values and to reduce nonspecific binding. Hence cysteine-capped NIR-emitting InP/ZnS core/shell NCs could be one of the best systems for biological *in vivo* studies provided they were sufficiently bright and stable. Therefore, the dramatic PL quenching of cysteine-capped InP/ZnS NCs is a major drawback as far as their bioapplications are concerned. We consistently observed the discussed behavior for different sized InP/ZnS NCs. Figure 4c shows the normalized PL of the QDs with the different ligands in water (pH 7.4). A slight red shift was observed (9 nm for MUA, 6 nm for DHLA, 15 nm for Cys, 3 nm for MPA, and 1 nm for TGA), which is attributed to the change of the dielectric environment and surface charge of the NCs.³⁶ In addition to the excitonic PL, peaking at 730 nm, we observe a shoulder at ~ 810 nm arising from the wavelength-dependent spectral response of the fluorometer.

Seen alone, the results obtained with Cys and DHLA imply that the thickness (~ 1 nm) and/or quality of the ZnS shell are not sufficient.¹⁰ On the other hand, the relatively large lattice mismatch of 7.6% between the InP core and the ZnS shell in the cubic phase impedes the growth of a defect-free, thicker shell. Therefore it is necessary to identify and eliminate the source of PL quenching at the NCs' surface. Both Cys and DHLA are susceptible to oxidation under disulfide formation in a solution of basic pH: in the case of DHLA an intramolecular reaction yielding thioacetic acid takes place; in the case of cysteine its dimer (cystine) is formed. Disulfide bonds are well known to quench the fluorescence of organic molecules such as tyrosine and tryptophan.³⁷

Moreover, the fluorescence of MPA-capped CdTe QDs is efficiently quenched in the presence of cysteine at pH > 9.6 .³⁸ The observed quenching has been attributed to hole transfer from the band edge (HOMO) of the QDs to the cysteine/cystine redox energy level. In the following we will restrict our discussion to cysteine; for DHLA the behavior is very similar (*cf.* Supporting Information). As discussed above, the phase transfer reaction with cysteine is carried out at pH 9.2 in order to obtain long-term colloidal stability. On the other hand, these conditions also favor cystine generation. When the as-transferred NCs were kept for 24 h without purification and removal of excess cysteine, we observed the formation of white crystals on the bottom of the vial (Supporting Information), while no precipitation of the NCs themselves could be detected. As expected for cysteine, the obtained crystals were insoluble in water, alcohol, chloroform, and acetone and could be solubilized in water only at elevated pH (> 10).³⁹ ^1H NMR analysis unambiguously confirmed the formation of cystine (Supporting Information). To further investigate the fluorescence quenching mechanism, we performed the phase transfer of InP/ZnS NCs with cysteine in the presence or absence of tris(2-carboxyethyl)phosphine hydrochloride, a molecule that is used for the selective reduction of disulfide bonds within a wide pH range. Remarkably, in the presence of TCEP 72% of the initial PL QY was retained (Figure 5a,b) with 730 nm emitting InP/ZnS NCs. The beneficial effect of TCEP on the QY was also observed when the quenched QDs (QY $< 0.5\%$) were *subsequently* treated with TCEP. Within 2 h, the fluorescence already increased 5-fold, and the



Scheme 2. Possible mechanisms taking place in the fluorescence quenching induced by hole (h^+) transfer from the QD to cystine and the PL recovery in the presence of tris(2-carboxyethyl)phosphine. In addition to being a reducing agent for cystine, TCEP and its oxidized form TCEPO can also act as the nanocrystals' surface ligands.

maximum increase was 13-fold when the solution was kept in the dark at room temperature for 72 h (Figure 5c). In other words, a substantial fraction of the PL intensity lost during the phase transfer using cysteine at pH \sim 9 could be recovered by means of the addition of the disulfide reducing agent TCEP.

In all experiments, the pH was kept constant (\sim 9) in order to rule out any pH-related changes in the PL emission. The amount of TCEP with respect to cysteine-capped QDs was chosen in a way that even if there were 100% of disulfide bond formation, still sufficient TCEP would be present to reduce them. The hypothetical mechanisms occurring during PL quenching and recovery are illustrated in Scheme 2: (1) hole transfer from the valence band of InP/ZnS NCs to cystine bound or in proximity to the surface, leading to fluorescence quenching; (2) cystine reduction by TCEP, while TCEP itself gets oxidized to TCEPO.⁴⁰

Both TCEP and TCEPO have functionalities (phosphine and phosphine oxide) that are known to passivate the surface of various types of semiconductor NCs, including InP,⁴¹ and to improve their photoluminescence efficiency. Therefore it is possible (even though not proven) in the present case that TCEP and/or TCEPO also act as surface ligands, completing the ligand sphere of the NCs and passivating surface trap states. Depending on the nature of QDs, different ligands show different quenching properties. For example, thiols such as amino-ethanethiol or hexanethiol give high quantum yields with CdTe NCs, while they quench almost completely the fluorescence of CdSe NCs.⁴² This behavior was attributed to the difference in the energetic position of the valence band of CdTe and CdSe with respect to the thiol redox level; in the case of CdSe,

the lower lying valence band edge leads to hole trapping on the thiols. In the other example cited earlier,³⁸ at pH $>$ 9.6 the addition of cysteine to MPA-capped CdTe NCs led to a pronounced drop in fluorescence. In contrast, no such quenching was observed with homocysteine, a homologue of cysteine with an additional methylene group. To date, no biological studies with cysteine-capped InP/ZnS NCs have been published despite the reported advantages of cysteine with CdSe-based QDs.^{10,11} One of the reasons could be the strong PL quenching of InP/ZnS NCs by cystine, which we have put into evidence here. Cystine can interact either directly with the QD surface through coordination bonding or with surface-bound cysteine molecules through electrostatic or H-bonding interactions. Therefore, despite the observed crystallization of cystine from excess cysteine, the interaction of a small fraction of this compound with the QDs cannot be excluded. We propose a 2-fold solution to this problem: (a) The first is the use of TCEP for preventing the dimerization of excess cysteine *during* the phase transfer. The most important factor here is the stronger binding of cysteine to the QD surface using our method as compared to reported procedures without pH control. As soon as excess cysteine is removed during the purification step, no further TCEP is required. Up to 94% of the initial quantum yield could be conserved for Cys-capped 660 nm emitting InP/ZnS NCs transferred in the presence of TCEP, and a decrease of less than 20% was observed during storage in the dark for more than two months. Under optimized conditions, the brightest NIR (740 nm) emitting Cys-capped InP/ZnS NCs exhibited a fluorescence quantum yield of 15% in 1 \times PBS buffer or water. These QDs have a high potential for *in vivo* biological studies.

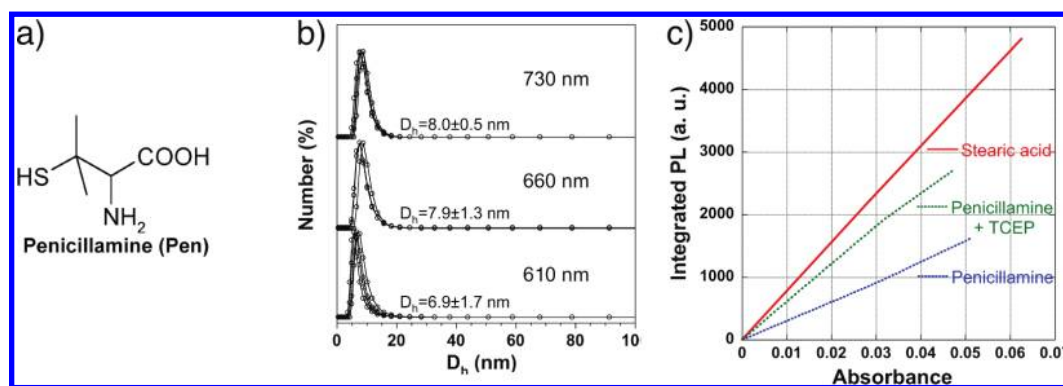


Figure 6. (a) Chemical structure of penicillamine. (b) Hydrodynamic diameter measurements of 610 nm, 660 nm, and 730 nm emitting InP/ZnS NCs in water directly after the phase transfer (ligand:QD ratio = 10^5). Multiple runs (>3) were performed for each sample. (c) Integrated photoluminescence vs absorbance plot for the 730 nm emitting NCs in the presence (green) and absence (blue) of TCEP during the phase transfer.

(b) The second solution is the use of penicillamine, providing similar properties to cysteine, such as being biocompatible, compact, and zwitterionic but being less prone to dimerization.

Penicillamine: A Suitable Substitute for Cysteine. In contrast to cysteine, penicillamine contains two methyl groups instead of protons at the carbon atom in α position to the thiol group (Figure 6a). This slight structural difference has a strong influence on the reactivity of both molecules. In particular, the sterically hindered thiol group in penicillamine makes it less susceptible to dimerization as compared to cysteine.⁴³ We note that cystine, the dimerization product of cysteine, is responsible for up to 4% of all kidney stones due to its insolubility at the pH prevalent in the kidneys.⁴⁴ Therefore, *in vivo* studies using InP/ZnS QDs capped with cysteine could presumably result in side effects related to insoluble cystine formation. Penicillamine, on the other hand, is used in the treatment of cystinuria, a genetic disease caused by accumulation of cystine in the kidneys.⁴⁵ In fact, penicillamine-cysteine disulfide has a much higher solubility at near-neutral pH values than cystine. In the literature penicillamine has been used as a capping ligand for the aqueous synthesis of QDs⁴⁶ and also as a phase transfer agent of CdSe/ZnS QDs at pH 7.4 in PBS buffer.²⁴ At pH 9 the phase transfer reaction takes place within 2 h, and after purification and transfer to $1 \times$ PBS buffer the QDs are stable for more than 10 weeks (Supporting Information). The transfer yield with penicillamine is similar to that obtained with cysteine (around 60%), while a more negative zeta potential (-32.7 vs -22.3 mV) is observed. The hydrodynamic diameters obtained for 610 nm (orange), 660 nm (red), and 730 nm (near-infrared) emitting InP/ZnS NCs in water are 6.9 ± 1.3 , 7.9 ± 1 , and 8 ± 0.5 nm, respectively (Figure 6b). In contrast to cysteine (retained QY 4%), with penicillamine as the phase transfer ligand the retained QY of the same InP/ZnS NCs is around 41% (Figure 6c). This

value agrees with the results obtained by Breus *et al.* on penicillamine-capped CdSe/ZnS NCs (40–60%)²⁴ and could further be improved up to $\sim 75\%$ for 730 nm emitting InP/ZnS NCs by adding TCEP during the phase transfer.

Versatility of the Phase Transfer Protocol. We evaluated the versatility of the phase transfer reaction by using QDs of various composition, size, and shape. In addition to different sized InP/ZnS NCs, our method relying on the precise adjusting of the pH depending on the chosen phase transfer ligand (cf. Table 1) was also successfully applied without any modification to spherical myristic acid-capped InP core NCs, tetradecylphosphonic acid/trioctylphosphine oxide-capped CdSe and CdSe/CdS nanorods, triangular shaped oleylamine-capped CuInS₂ NCs, spherical stearic acid/oleylamine-capped CdSe/CdS/ZnS, and dodecanethiol-capped CuInS₂/ZnS core/shell structures (cf. Figure 7). It must be noted, however, that the transfer yield strongly depends on the initial surface ligands. In the case of NCs already capped with thiols it was much lower (<30%) than in the case of fatty acid- and/or amine-capped QDs (50–98%). In this context, it has been shown that the precise determination of the nature of the initial surface ligands is complicated by the presence of byproducts, such as *n*-octylphosphonate in technical grade trioctylphosphine oxide⁴⁷ and dioctylphosphine in commonly used 90% trioctylphosphine.⁴⁸ Concerning the retained PL QY, a clear correlation with the QD composition and presence of a ZnS shell is visible. As mentioned above, the fluorescence of core CdSe NCs is easily quenched by thiols,⁴² and indeed the PL intensity of CdSe nanorods decreased by more than 2 orders of magnitude upon phase transfer with cysteine (Figure 7c). The same applies to spherical core InP NCs. Adding a CdS shell to CdSe nanorods (Figure 7d) significantly increases the amount of retained PL efficiency. Even though the conduction band offset with CdSe is much smaller than in the case of a ZnS shell,

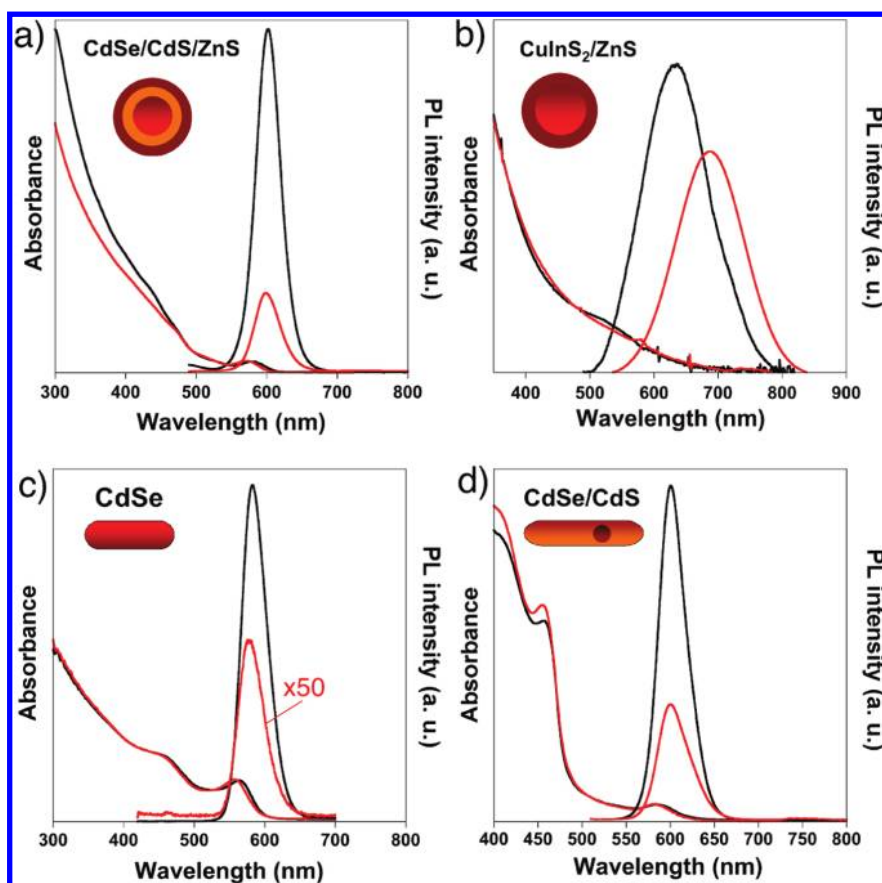


Figure 7. UV-vis and PL spectra of different types of NCs before and after phase transfer using the standard procedure without addition of TCEP. (a) ~ 6 nm CdSe/CdS/ZnS cores/shell/shell NCs capped with penicillamine; (b) ~ 7 nm CuInS₂/ZnS core/shell NCs capped with MUA; (c) $\sim 3.5 \times 15$ nm CdSe nanorods capped with cysteine; and (d) $\sim 4 \times 32$ nm CdSe/CdS nanorods with penicillamine. Red lines: spectra recorded in water, black lines: spectra in organic phase (hexanes or chloroform); the absorbance of the samples before and after phase transfer was adjusted to be equal at the PL excitation wavelength.

CdS provides nonetheless a large valence band offset. Thus depending on the barrier (=shell) thickness, hole trapping by surface ligands is strongly reduced. Nevertheless, when no TCEP is added during the transfer of CdSe/CdS nanorods with penicillamine, the integrated PL intensity drops to 39% of its initial value in organic solvent. This decrease is even more pronounced (retained PL 25%) in the case of CdSe/CdS/ZnS NCs using the same ligand (Figure 7a). For CuInS₂/ZnS QDs 76% of the initial PL QY is retained when transferring with MUA to the aqueous phase. At the same time a pronounced bathochromic shift of the PL peak from 632 to 688 nm is observed. In contrast to the excitonic band edge emission exhibiting systems discussed above, the emission in CuInS₂-based NCs relies on a different mechanism. It takes place *via* transitions from the conduction band to surface- and/or volume-related acceptor states.^{49,50} Depending on their energetic level positions with respect to surface thiols or disulfides, hole transfer may be energetically unfavorable, which could explain the high retained PL efficiency in this case.

CONCLUSION

We presented an aqueous phase transfer procedure for colloidal InP/ZnS quantum dots based on the use of readily available, small, hydrosoluble thiols. The deprotonation of the thiol function by the appropriate adjustment of the pH of the aqueous phase is important to obtain strong binding of the ligand molecules to the NCs' surface. Using this approach cysteine and penicillamine-capped InP/ZnS NCs with a colloidal stability of several weeks in water or buffer solution have been obtained. They combine a low hydrodynamic diameter (<10 nm) and potentially low nonspecific binding in biological environments due to their zwitterionic coating. The developed strategy can be applied for a large variety of QDs and NPs whose surface atoms have an affinity for thiolates. The formation of cysteine dimer, cystine, has been shown to be at the origin of the significant decrease of the PL efficiency of phase-transferred cysteine-capped InP/ZnS QDs. This phenomenon can be avoided by addition of the reducing agent TCEP during the transfer reaction, and in the best cases more than 90% of the initial fluorescence intensity can be retained.

We expect that these results open up the way for taking advantage of the full potential of InP/ZnS NCs

as fluorescent labels for biological *in vitro* and *in vivo* studies.

METHODS

Materials. D-Penicillamine, L-cysteine, thioglycolic acid (98%), 11-mercaptoundecanoic acid (95%), tetramethylammonium hydroxide (97%), phosphate-buffered saline solution (1× PBS), 3-mercaptopropanoic acid (99+%), and tris(2-carboxyethyl) phosphine hydrochloride solution (0.5 M) were purchased from Sigma-Aldrich and used as received. Dihydrolipoic acid was synthesized from thioacetic acid following a literature procedure.⁵¹

Instruments. UV–vis absorption spectra were recorded on a HP 8452A spectrometer; photoluminescence (PL) spectra on a Hitachi F-4500 spectrofluorometer. Fluorescence quantum yields were determined by comparison of the integrated fluorescence intensity of a NCs' dispersion with that of a standard of known QY (rhodamine 6G in ethanol, QY = 95%). Both the sample and the reference were excited at 480 nm. The measurements were repeated for multiple (>3) concentrations in order to increase the accuracy. By comparing the slopes of the resulting linear absorbance vs PL intensity plots and correcting for the solvent refractive indices, the QY was obtained. The hydrodynamic diameter of the water-soluble NCs dispersed in water was measured by dynamic light scattering, using a Malvern Zeta Sizer (NanoZS). The samples have been thoroughly purified with centrifugal filters from VWR (MWCO 30k) and dispersed in Milli-Q water (18 mΩ) prior to the measurements. For the long-term colloidal stability tests in electrolytic environment 1× PBS buffer is used instead of water. Given the sensitivity of the instrument, multiple runs (>3) were performed to avoid erroneous results. The spectra have been corrected by the instrument software for viscosity (0.882 mPa·s at 25 °C), absorption (at 532 nm), solvent (water) refractive index (1.33), and material (InP) refractive index (3.1). The data are collected in automatic mode and expressed in number %. The zeta potential is measured in the same instrument but under zeta potential settings. Chirality measurements were performed with a Chirascan CD spectropolarimeter. The used Pen-capped InP/ZnS NCs were passed through Nap5 size exclusion columns from GE-Biosciences and dispersed in 1× PBS buffer prior to the measurements.

Phase Transfer of QDs. *Purification.* Thorough purification of the initial QDs assuring the removal of excess hydrophobic ligands is crucial for the successful phase transfer. A 5 mL amount of the QDs in organic solvent is mixed with anhydrous ethanol (1:3) and centrifuged at 10 000 rpm (rotations per minute) for 6 min. The clear solution of supernatant is discarded, and the precipitate is redispersed in 15 mL of a 1:3 chloroform/ethanol mixture and centrifuged again. The precipitate is dispersed in a minimum amount of chloroform. The concentration is estimated from the first excitonic peak in the UV–vis spectrum.¹⁷

Phase Transfer. Typically a 0.2 M solution of the ligand is prepared in 1 mL of degassed Milli-Q water (18 MΩ), and the pH is adjusted to the value specified in Table 1 by dropwise addition of 0.5 M tetramethylammonium hydroxide. This solution is mixed with 1.5 mL of a ~5 μM dispersion of the QDs in chloroform. The biphasic mixture is stirred vigorously at 1400 rpm for 2 h.

Phase Transfer in the Presence of TCEP. The same procedure as before is applied with the difference that the ligand solution is constituted of 500 μL of a 0.2 M solution of the transfer ligand and 100 μL of a 0.5 M TCEP solution, mixed with 1 mL of ~5 μM dispersion of QDs in chloroform.

Workup. Depending on the nature of the initial ligands on the QDs surface in organic media, at the end of the reaction the biphasic mixture can result in the clear separation of two phases or in an emulsion. In the latter case, the mixture is centrifuged at lower speed (6000 rpm) for 1 min to obtain a clear phase

separation. The QDs in the (upper) aqueous phase are separated from the (lower) organic phase.

Purification and Storage. A 200 μL amount of the QDs in water is centrifuged in a Millipore centrifugal filter from VWR (MWCO 30k) at 10 000 rpm for 2 min. Then 200 μL of 1× PBS buffer (pH 7.4) or Milli-Q water is added to the pellet, and the QDs are redispersed in 200 μL of 1× PBS buffer or Milli-Q water (pH ~7) and stored in a refrigerator (4 °C). The typical storage concentration is around 10 μM. Alternatively, the QDs can be purified by using NAP-5 size exclusion columns from GE-Biosciences.⁴⁹

Recovery of Fluorescence by Addition of TCEP. A 600 μL sample of a ~6 μM dispersion of freshly transferred cysteine-capped InP/ZnS NCs at pH 9 is mixed with 100 μL of a 0.5 M TCEP solution.

Quantum Dot Synthesis. *Synthesis of InP/ZnS NCs.* The synthesis of InP/ZnS NCs emitting at wavelengths of >700 nm is based on a procedure we reported earlier.²¹ In brief, the indium precursor (1 equiv of indium myristate in 1-octadecene) was reacted under an Ar atmosphere with *in situ* generated PH₃ gas at 250 °C for 60 min to form the core InP NCs. For growth of the ZnS shell, 10 equiv of zinc stearate is added into the dispersion of the InP NCs and heated to 280 °C to form a Zn²⁺-rich surface before injecting slowly 2.5 equiv of zinc ethylxanthate at 210 °C to grow ZnS. The 610 nm emitting InP QDs were synthesized following the procedure of Xu *et al.*²³ The 660 nm emitting QDs are prepared using the same protocol, except that *in situ* generated PH₃ gas was used instead of P(TMS)₃ as the phosphorus precursor: indium(III) acetate (1 equiv) in 1-octadecene is reacted with PH₃ gas at 250 °C in the presence of stearic acid (1 equiv), hexadecylamine (2 equiv), and zinc undecylate (1 equiv).

Synthesis of Other Types of QDs. The synthesis of other types of QDs followed reported protocols: CdSe/CdS core/shell nanorods,⁵² CdSe nanorods,⁵³ CdSe/CdS/ZnS core/shell/shell NCs,⁵⁴ tetragonal CuInSe₂,⁵⁵ and CuInS₂/ZnS core/shell NCs.⁴⁹

Acknowledgment. This article is dedicated to Prof. A. Pron on the occasion of his 60th birthday. The presented research was financially supported by the French Research Agency (ANR-PNANO-07-044: SYNERGIE) and by the CEA Program Technologies pour la Santé (TIMOMA2). We thank E. Rossitto, M. Protière, L. Hartmann, N. Nerambourg, L. Li, and A. Fiore for providing CdSe/CdS core/shell nanorods, CdSe nanospheres and nanorods, and CdSe/CdS/ZnS, CuInS₂/ZnS, and CuInSe₂ QDs, respectively. We gratefully acknowledge J. Gravier for DLS measurements, as well as T. J. Daou, G. Stasiuk, and A. Chassin De Kergommeaux for helpful discussions.

Supporting Information Available: Titration curves of the phase transfer ligands, NMR spectra, fluorescence recovery of DHLA-capped QDs, and hydrodynamic diameter measurements of Pen-capped QDs. This information is available free of charge via the Internet at <http://pubs.acs.org>.

REFERENCES AND NOTES

- Bruchez, M.; Moronne, M.; Gin, P.; Weiss, S.; Alivisatos, A. P. Semiconductor Nanocrystals as Fluorescent Biological Labels. *Science* **1998**, *281*, 2013–2016.
- Chan, W. C. W.; Nie, S. M. Quantum Dot Bioconjugates for Ultrasensitive Nonisotopic Detection. *Science* **1998**, *281*, 2016–2018.
- Medintz, I. L.; Uyeda, H. T.; Goldman, E. R.; Mattoussi, H. Quantum Dot Bioconjugates for Imaging, Labelling and Sensing. *Nat. Mater.* **2005**, *4*, 435–446.
- Doty, R. C.; Tshikhudo, T. R.; Brust, M.; Fernig, D. G. Extremely Stable Water-Soluble Ag Nanoparticles. *Chem. Mater.* **2005**, *17*, 4630–4635.

5. Susumu, K.; Uyeda, H. T.; Medintz, I. L.; Pons, T.; Delehanty, J. B.; Mattoussi, H. Enhancing the Stability and Biological Functionalities of Quantum Dots Via Compact Multifunctional Ligands. *J. Am. Chem. Soc.* **2007**, *129*, 13987–13996.
6. Roullier, V.; Clarke, S.; You, C.; Pinaud, F.; Gouzer, G.; Schaible, D.; Marchi-Artzner, V.; Piehler, J.; Dahan, M. High-Affinity Labeling and Tracking of Individual Histidine-Tagged Proteins in Live Cells Using Ni²⁺ Tris-Nitrilotriacetic Acid Quantum Dot Conjugates. *Nano Lett.* **2009**, *9*, 1228–1234.
7. Lévy, R.; Thanh, N. T. K.; Doty, R. C.; Hussain, I.; Nichols, R. J.; Schiffrin, D. J.; Brust, M.; Fernig, D. G. Rational and Combinatorial Design of Peptide Capping Ligands for Gold Nanoparticles. *J. Am. Chem. Soc.* **2004**, *126*, 10076–10084.
8. Dubertret, B.; Skourides, P.; Norris, D. J.; Noireaux, V.; Brivanlou, A. H.; Libchaber, A. In Vivo Imaging of Quantum Dots Encapsulated in Phospholipid Micelles. *Science* **2002**, *298*, 1759–1762.
9. Pellegrino, T.; Manna, L.; Kudera, S.; Liedl, T.; Koktysh, D.; Rogach, A. L.; Keller, S.; Radler, J.; Natile, G.; Parak, W. J. Hydrophobic Nanocrystals Coated with an Amphiphilic Polymer Shell: A General Route to Water Soluble Nanocrystals. *Nano Lett.* **2004**, *4*, 703–707.
10. Choi, H. S.; Liu, W.; Misra, P.; Tanaka, E.; Zimmer, J. P.; Ipe, B. I.; Bawendi, M. G.; Frangioni, J. V. Renal Clearance of Quantum Dots. *Nat. Biotechnol.* **2007**, *25*, 1165–1170.
11. Liu, W.; Choi, H. S.; Zimmer, J. P.; Tanaka, E.; Frangioni, J. V.; Bawendi, M. Compact Cysteine-Coated CdSe(ZnCdS) Quantum Dots for in Vivo Applications. *J. Am. Chem. Soc.* **2007**, *129*, 14530–14531.
12. Pinaud, F.; Clarke, S.; Sittner, A.; Dahan, M. Probing Cellular Events, One Quantum Dot at a Time. *Nat. Methods* **2010**, *7*, 275–285.
13. Zimmer, J. P.; Kim, S. W.; Ohnishi, S.; Tanaka, E.; Frangioni, J. V.; Bawendi, M. G. Size Series of Small Indium Arsenide-Zinc Selenide Core-Shell Nanocrystals and Their Application to in Vivo Imaging. *J. Am. Chem. Soc.* **2006**, *128*, 2526–2527.
14. Liu, D.; Snee, P. T. Water-Soluble Semiconductor Nanocrystals Cap Exchanged with Metalated Ligands. *ACS Nano* **2010**, *5*, 546–550.
15. Breus, V. V.; Heyes, C. D.; Nienhaus, G. U. Quenching of CdSe/ZnS Core/Shell Quantum Dot Luminescence by Water-Soluble Thiolated Ligands. *J. Phys. Chem. C* **2007**, *111*, 18589–18594.
16. Yong, K.-T.; Ding, H.; Roy, I.; Law, W.-C.; Bergey, E. J.; Maitra, A.; Prasad, P. N. Imaging Pancreatic Cancer Using Bioconjugated InP Quantum Dots. *ACS Nano* **2009**, *3*, 502–510.
17. Peng, X. G.; Schlamp, M. C.; Kadavanich, A. V.; Alivisatos, A. P. Epitaxial Growth of Highly Luminescent CdSe/CdS Core/Shell Nanocrystals with Photostability and Electronic Accessibility. *J. Am. Chem. Soc.* **1997**, *119*, 7019–7029.
18. Reiss, P.; Bleuse, J.; Pron, A. Highly Luminescent CdSe/ZnSe Core/Shell Nanocrystals of Low Size Dispersion. *Nano Lett.* **2002**, *2*, 781–784.
19. Mekis, I.; Talapin, D. V.; Kornowski, A.; Haase, M.; Weller, H. One-Pot Synthesis of Highly Luminescent CdSe/CdS Core-Shell Nanocrystals Via Organometallic and "Greener" Chemical Approaches. *J. Phys. Chem. B* **2003**, *107*, 7454–7462.
20. Xie, R.; Battaglia, D.; Peng, X. Colloidal InP Nanocrystals as Efficient Emitters Covering Blue to Near-Infrared. *J. Am. Chem. Soc.* **2007**, *129*, 15432–15433.
21. Li, L.; Protière, M.; Reiss, P. Economic Synthesis of High Quality InP Nanocrystals Using Calcium Phosphide as the Phosphorus Precursor. *Chem. Mater.* **2008**, *20*, 2621–2623.
22. Li, L.; Reiss, P. One-Pot Synthesis of Highly Luminescent InP/ZnS Nanocrystals without Precursor Injection. *J. Am. Chem. Soc.* **2008**, *130*, 11588–11589.
23. Xu, S.; Ziegler, J.; Nann, T. Rapid Synthesis of Highly Luminescent InP and InP/ZnS Nanocrystals. *J. Mater. Chem.* **2008**, *18*, 2653–2656.
24. Breus, V. V.; Heyes, C. D.; Tron, K.; Nienhaus, G. U. Zwitterionic Biocompatible Quantum Dots for Wide pH Stability and Weak Nonspecific Binding to Cells. *ACS Nano* **2009**, *3*, 2573–2580.
25. Schapotschnikow, P.; Hommersom, B.; Vlucht, T. J. H. Adsorption and Binding of Ligands to CdSe Nanocrystals. *J. Phys. Chem. C* **2009**, *113*, 12690–12698.
26. Pong, B.-K.; Trout, B. L.; Lee, J.-Y. Modified Ligand-Exchange for Efficient Solubilization of CdSe/ZnS Quantum Dots in Water: A Procedure Guided by Computational Studies. *Langmuir* **2008**, *24*, 5270–5276.
27. Fritzinger, B.; Moreels, I.; Lommens, P.; Koole, R.; Hens, Z.; Martins, J. C. In Situ Observation of Rapid Ligand Exchange in Colloidal Nanocrystal Suspensions Using Transfer NOE Nuclear Magnetic Resonance Spectroscopy. *J. Am. Chem. Soc.* **2009**, *131*, 3024–3032.
28. Pine, S. H. *Organic Chemistry*, 5th ed.; MacGraw-Hill: New York, 1987.
29. Algar, W. R.; Krull, U. J. Luminescence and Stability of Aqueous Thioalkyl Acid Capped CdSe/ZnS Quantum Dots Correlated to Ligand Ionization. *ChemPhysChem* **2007**, *8*, 561–568.
30. Li, N. C.; Manning, R. A. Some Metal Complexes of Sulfur-Containing Amino Acids. *J. Am. Chem. Soc.* **1955**, *77*, 5225–5228.
31. Llinas, A.; Donoso, J.; Vilanova, B.; Frau, J.; Munoz, F.; Page, M. I. Thiol-Catalysed Hydrolysis of Benzylpenicillin. *J. Chem. Soc., Perkin Trans. 2* **2000**, 1521–1525.
32. Fauconnier, N.; Pons, J. N.; Roger, J.; Bee, A. Thiolation of Maghemite Nanoparticles by Dimercaptosuccinic Acid. *J. Colloid Interface Sci.* **1997**, *194*, 427–433.
33. Flanagan, R. J.; Jones, A. L. *Antidotes*, 1st ed.; Taylor&Francis: London, 2001.
34. Reiss, P.; Protière, M.; Li, L. Core/Shell Semiconductor Nanocrystals. *Small* **2009**, *5*, 154–168.
35. Parak, W. J.; Pellegrino, T.; Plank, C. Labelling of Cells with Quantum Dots. *Nanotechnology* **2005**, *16*, R9.
36. Thuy, U. T. D.; Liem, N. Q.; Thanh, D. X.; Protière, M.; Reiss, P. Optical Transitions in Polarized CdSe, CdSe/ZnSe, and CdSe/CdS/ZnS Quantum Dots Dispersed in Various Polar Solvents. *Appl. Phys. Lett.* **2007**, *91*, 241908.
37. Ross, J. B. A.; Laws, W. R.; Rousslang, K. W.; Wyssbrod, H. R. *Topics in Fluorescence Spectroscopy*; Lakowicz, J. R., Ed.; Plenum Press: New York, 1992; Vol. 3; pp 1–63.
38. Xia, Y.-S.; Zhu, C.-Q. Interaction of CdTe Nanocrystals with Thiol-Containing Amino Acids at Different pH: A Fluorimetric Study. *Microchim. Acta* **2009**, *164*, 29–34.
39. Carta, R.; Tola, G. Solubilities of L-Cystine, L-Tyrosine, L-Leucine, and Glycine in Aqueous Solutions at Various pHs and NaCl Concentrations. *J. Chem. Eng. Data* **1996**, *41*, 414–417.
40. Burns, J. A.; Butler, J. C.; Moran, J.; Whitesides, G. M. Selective Reduction of Disulfides by Tris(2-Carboxyethyl)-Phosphine. *J. Org. Chem.* **1991**, *56*, 2648–2650.
41. Guzelian, A. A.; Katari, J. E. B.; Kadavanich, A. V.; Banin, U.; Hamad, K.; Juban, E.; Alivisatos, A. P.; Wolters, R. H.; Arnold, C. C.; Heath, J. R. Synthesis of Size-Selected, Surface-Passivated InP Nanocrystals. *J. Phys. Chem.* **1996**, *100*, 7212–7219.
42. Wuister, S. F.; de Mello Donega, C.; Meijerink, A. Influence of Thiol Capping on the Exciton Luminescence and Decay Kinetics of CdTe and CdSe Quantum Dots. *J. Phys. Chem. B* **2004**, *108*, 17393–17397.
43. van de Stadt, R. J.; Muijsers, A. O.; Henrichs, A. M. A.; van der Korst, J. K. D-Penicillamine: Biochemical, Metabolic and Pharmacological Aspects. *Scand. J. Rheumat.* **1979**, *8*, 13–20.
44. Königsberger, E.; Wang, Z.; Königsberger, L.-C. Solubility of L-Cystine in NaCl and Artificial Urine Solutions. *Monatsh. Chem.* **2000**, *131*, 39–45.
45. Crawhall, J. C.; Thompson, C. J. Cystinuria: Effect of D-Penicillamine on Plasma and Urinary Cystine Concentrations. *Science* **1965**, *147*, 1459–1460.
46. Moloney, M. P.; Gun'ko, Y. K.; Kelly, J. M. Chiral Highly Luminescent CdS Quantum Dots. *Chem. Commun.* **2007**, 3900–3902.
47. Morris-Cohen, A. J.; Donakowski, M. D.; Knowles, K. E.; Weiss, E. A. The Effect of a Common Purification Procedure on the Chemical Composition of the Surfaces of CdSe

- Quantum Dots Synthesized with Trioctylphosphine Oxide. *J. Phys. Chem. C* **2009**, *114*, 897–906.
48. Evans, C. M.; Evans, M. E.; Krauss, T. D. Mysteries of TOPSe Revealed: Insights into Quantum Dot Nucleation. *J. Am. Chem. Soc.* **2010**, *132*, 10973–10975.
 49. Li, L.; Daou, T.; Texier, I.; Tran, T.; Liem, N.; Reiss, P. Highly Luminescent $\text{CuInS}_2/\text{ZnS}$ Core/Shell Nanocrystals: Cadmium-Free Quantum Dots for in Vivo Imaging. *Chem. Mater.* **2009**, *21*, 2422–2429.
 50. Li, L.; Pandey, A.; Werder, D. J.; Khanal, B. P.; Pietryga, J. M.; Klimov, V. I. Efficient Synthesis of Highly Luminescent Copper Indium Sulfide-Based Core/Shell Nanocrystals with Surprisingly Long-Lived Emission. *J. Am. Chem. Soc.* **2011**, *133*, 1176–1179.
 51. Clapp, A. R.; Goldman, E. R.; Mattoussi, H. Capping of CdSe-ZnS Quantum Dots with DHLA and Subsequent Conjugation with Proteins. *Nat. Prot.* **2006**, *1*, 1258–1266.
 52. Carbone, L.; Nobile, C.; De Giorg, M.; Sala, F. D.; Morello, G.; Pompa, P.; Hytch, M.; Snoeck, E.; Fiore, A.; Franchini, I. R.; *et al.* Synthesis and Micrometer-Scale Assembly of Colloidal CdSe/CdS Nanorods Prepared by a Seeded Growth Approach. *Nano Lett.* **2007**, *7*, 2942–2950.
 53. Shieh, F.; Saunders, A. E.; Korgel, B. A. General Shape Control of Colloidal CdS, CdSe, CdTe Quantum Rods and Quantum Rod Heterostructures. *J. Phys. Chem. B* **2005**, *109*, 8538–8542.
 54. Protiere, M.; Nerambourg, N.; Renard, O.; Reiss, P. Rational Design of the Gram-Scale Synthesis of Nearly Monodisperse Semiconductor Nanocrystals. *Nanoscale Res. Lett.* **2011**, *6*, 472.
 55. Koo, B.; Patel, R. N.; Korgel, B. A. Synthesis of CuInSe_2 Nanocrystals with Trigonal Pyramidal Shape. *J. Am. Chem. Soc.* **2009**, *131*, 3134–3135.